

Epidemic Dynamics via Wavelet Theory and Machine Learning, with Applications to Covid-19*

Tô Tat Dat[†], Protin Frédéric, Nguyen T.T. Hang,
 Martel Jules[‡], Nguyen Duc Thang, Charles Piffault, Rodríguez Willy,
 Figueroa Susely, Hông Vân Lê[§], Wilderich Tuschmann, Nguyen Tien Zung

Abstract

We introduce the concept of epidemic-fitted wavelets which comprise, in particular, as special cases the number $I(t)$ of infectious individuals at time t in classical SIR models and their derivatives. We present a novel method for modelling epidemic dynamics by a model selection method using wavelet theory and, for its applications, machine learning based curve fitting techniques. Our universal models are functions that are finite linear combinations of epidemic-fitted wavelets. We apply our method by modelling and forecasting, based on the John Hopkins University dataset, the spread of the current Covid-19 (SARS-CoV-2) epidemic in France, Germany, Italy and the Czech Republic, as well as in the US federal states New York and Florida.

Keywords: epidemic-fitted wavelet, epidemic dynamics, model selection, curve fitting, Covid-19 spread predicting.

1 Introduction

The present work proposes a novel method for modelling epidemic dynamics by combining wavelet theory and data-driven model section techniques in machine learning.

In understanding epidemic diffusion and growth rate of an infectious disease at population level, the actual number of reported cases of infections always plays a (if not even *the*) crucial role - and, way beyond that, at least in the case of diseases afflicting human societies, directly influences government and health care system decisions and measures regarding, e.g., protection, containment and hospital capacities.

*This work is supported by Torus Actions and Belle Artificial Intelligence Corporation

[†]corresponding author: tat-dat.to@imj-prg.fr

[‡]Invited fellow at Max Planck Institute, Bonn

[§]partially supported by GACR-project 18-01953J and RVO: 67985840

However, due to both the manifold practical as well as conceptual issues involved, a rigorous and accurate detection of this number turns out to be a rather difficult and complex problem.

To illustrate at least some of the theoretical difficulties involved here by a prominent and important case which calls the entire world now to action, let us note that most current mathematical modelling and forecasting techniques for the spread of the Covid-19 disease are based on classical SIR (Susceptible - Infectious - Recovered/Removed) and SEIR (Susceptible - Exposed - Infectious - Recovered/Removed) compartmental epidemiological models [24, 6, 49].

Yet, with regard to predicting the number of infectious cases $I(t)$ at time t , they suffer from severe and model-inherent principal limitations:

All these models, as well as all their derivatives, are not suitable to build a model for the function $I(t)$ which is compatible with any given population. This is because these models are based on the assumption that the population is homogeneously composed and distributed (i.e., the chance that an arbitrary infected person will infect an arbitrary susceptible person is taken to be constant throughout the epidemic, and, moreover, it is assumed that at any given time every infected person has one and the same constant chance to recover).

In real life, however, there are actually many and rather diverse waves of outbreaks, stemming from different times or locations. One faces here not only drastically varying growth rates, but also hot spots versus no-cluster locations, infection rates depending on age or other parameters, etc. which altogether entails that the homogeneity assumption approach taken in SIR models and their variations is over-simplified and cannot give realistic forecasts.

To overcome the draw-backs caused by homogeneity assumptions, the new approach presented in this work is based on the following idea: we shall decompose the growth curve of infection numbers into several basic 'waves', where each basic wave is considered as a representation of the epidemic, and localised both in time and position.

This point of view naturally calls for the use of wavelet theory. Wavelets as such are special families of functions which came up in the 1980s by combining older concepts from mathematics, computer science, electrical engineering and physics, having since then found fruitful applications in many other disciplines. In particular, some precursor, wave-based approaches to modelling epidemic growth appeared already a long time before wavelets emerged in both deterministic and stochastic models, compare, among others, [46, 3, 4, 28], and only very recently, Krantz et al. (compare [27]) Moreover, the latter work has also proposed building epidemic growth models by combining wavelet with discrete graph theory (see also below).

In this article, we propose an approach to epidemic dynamics by modelling the number of daily reported cases using specially designed wavelets, called epidemic-fitted (EF) wavelets.

For instance, the number $I(t)$ of infectious individuals at time t in the classical SIR and SEIR models is an EF wavelet, see Subsection 3.4. Another example of an EF wavelet is the log-normal one, which we will use in our Covid-19 spread forecasting

applications, see subsections 4.1, 3.4 for more details.

In our approach, the number of daily reported cases is the value of a function that is a positive linear combination of N EF wavelets at the given day. We fix the number N of summands of EF wavelets entering in our modelling function (and in our applications N is usually taken to be 3 or 5). The wavelet series coefficients themselves are then obtained by machine learning based curve fitting methods with square loss function, see subsections 2.2 and 4.1.

We then proceed with specific applications to Covid-19 scenarios. Here we present, now using in addition data-driven machine learning based curve fitting, some of our model's predictions to selected countries and US federal states, which are based on the currently existing respective data for these locations provided by the most recent numbers supplied by the Johns Hopkins University Covid-19 database.

Before mentioning and commenting upon other related works, let us adopt from now on, and throughout all following parts of the present work, the following *convention*: as we shall consider only reported cases in our paper, we will omit the adjective 'reported' from 'reported cases of infected'.

In [5], the authors present three basic 'macroscopic' models to fit data emerging from local and national governments: exponential growth, self-exciting branching process and compartmental models. The compartmental models are the classical SIR and SEIR models, the self-exciting branching process has been used before with regard to treating Ebola disease outbreaks and other dynamics of social interaction. In the exponential growth model, the number $I(t)$ of infectious individuals at time t is expressed as $I(t) = I_0 e^{\alpha t}$, where α is the rate constant. The exponential growth model is related to our approach, in which the exponential function is modelling the reported infections. However, since this is a one-parameter model, it works only well for fitting the data at the beginning of an outbreak.

In [34] the authors use a log-normal density function with three parameters to fit the daily reported cases. But since they tried to fit the data with only one function, the curve of reported cases may not be well fitted, since there are usually several waves of the epidemic for a period while one function presents only one wave. As explained above, our wavelet approach does overcome this difficulty.

In [48], the authors use the function $f(x) = k \cdot \gamma \cdot \beta \cdot \alpha^\beta \cdot x^{-1-\beta} \cdot \exp(-\gamma(\alpha/x)^\beta)$ to fit all data. This method, too, can fit the data only for one wave.

In [12] the authors fit the data of daily reported cases with a two-wave model, using the sum of two Gaussian functions.

In [9], the authors introduce an epidemic model composed of overlapping sub-epidemic waves, where each single one is a generalized logistic growth model given by solution of differential equations. A short term forecast of the Covid-19 epidemic in China from February 5th to February 24th was given in [41] using three phenomenological models (generalized logistic growth model, the Richards growth model, sub-epidemic wave model in [9]) and ensemble methods (see also [10] for the ensemble approach in forecasting epidemic trajectories).

In [25], a multi-wave model combining several SIR models, namely, a Multiple-Wave Forced-SIR model, was introduced to fit the data of daily cases.

Recently, Krantz et al. [27] have proposed an approach to construct epidemic growth models using *fractional* wavelets. These are built from the number of reported cases to construct wavelets that model the dynamics of the number of completed cases ([27]). In their paper, the number of completed cases is the sum of the number of reported cases and the number of unreported cases. Furthermore, the proposed approach there is to update their models assuming the availability of the reporting error which improves over time and tends to zero eventually. This assumption appears to us, however, as a too idealistic one.

Those two last approaches are the ones which are most closely related to our own. However, while those use single waves coming from solutions differential equations, we use general wavelet functions such as Gaussian functions, log-normal functions, Gompertz density functions, and Beta prime density functions, which all satisfy our general condition of being epidemic-fitted in the sense of Definition 2.

We also refer to [15, 16, 20, 53, 18, 52, 40, 2, 29, 14, 42, 35, 22, 1, 26, 19, 51, 54, 31, 32, 33, 11, 43, 44] for other approaches on modelling and forecasting the spread of Covid-19 epidemic using deep learning, machine learning, time series analysis, network model, stochastic model and deterministic compartmental framework.

The remaining parts of the present paper are organized as follows:

In section 2 we first recall the notion of a wavelet (Definition 1) and the fundamental theorem of wavelet theory (Theorem 1) which we are going to put to use in the sequel. We proceed by introducing the notion of an epidemic-fitted (EF) wavelet (Definition 2) and propose our method for modelling epidemic dynamics (Proposition 1), justified by the fundamental theorem 1. In Section 3 we consider several important examples of EF wavelets and impose constraints on an EF wavelet to be suitable as a basic EF wavelet in epidemic dynamics. In Section 4 we present applications of our method to modelling and forecasting the current spread of Covid-19 in France, Germany, Italy, the Czech Republic and several US federal states, all based on the most recent JHU data.

Acknowledgement. It is our pleasure to thank Tat Dat Tran and Vit Fojtik for useful suggestions and comments on an earlier version of this paper.

2 Epidemic Modelling via Wavelet Theory and Machine Learning

2.1 Wavelets

In this subsection, we recall and collect some basic concepts and facts from Wavelet Theory (cf. [13, 38, 39]), which will be needed in our approach for modelling epidemic dynamics.

Definition 1 [13, p.24] A wavelet or (mother wavelet) is a function $\psi \in L^1(\mathbb{R})$ such that the following admissibility condition holds:

$$C_\psi = \int_{-\infty}^{\infty} |\hat{\psi}(\xi)|^2 \frac{d\xi}{|\xi|} < \infty, \quad (1)$$

where $\hat{\psi}$ is the Fourier transform of ψ , i.e., $\hat{\psi}(\xi) = \int_{\mathbb{R}} \psi(x)e^{-i\xi x} dx$.

Notice that condition (1) is only satisfied if $\hat{\psi}(0) = 0$ or $\int \psi(x)dx = 0$. Conversely, we have the following sufficient condition for (1).

Lemma 1 [13, p.24] Let $\psi \in L^1(\mathbb{R})$ and $\int_{\mathbb{R}} \psi(x)dx = 0$. If $\int_{\mathbb{R}} |\psi(x)|(1 + |x|)^\alpha dx < \infty$ for some $\alpha > 0$, then $|\hat{\psi}(\xi)| \leq C|\xi|^{\min(\alpha, 1)}$ and $C_\psi < \infty$.

A basic example of a wavelet is the function

$$\psi(t) = \frac{\sin(2\pi t) - \sin(\pi t)}{\pi t}.$$

From a mother wavelet one can generate other wavelets (called *children wavelets*), using affine transformations (i.e., dilations and translations):

$$\psi_{a,b}(t) = \frac{1}{\sqrt{|a|}} \psi\left(\frac{t-b}{a}\right), \quad (a, b) \in \mathbb{R} \times \mathbb{R}.$$

These wavelets provide us with the following decomposition of $L^2(\mathbb{R})$:

Theorem 1 [13, Proposition 2.4.1 and p. 25-26] Let ψ be a mother wavelet. Then any $f \in L^2(\mathbb{R})$ decomposes as

$$f = C_\psi^{-1} \int_{\mathbb{R}^2} \langle f, \psi_{a,b} \rangle \psi_{a,b} \frac{dad b}{a^2}, \quad (2)$$

strongly in $L^2(\mathbb{R})$, where \langle, \rangle denotes the standard product in $L^2(\mathbb{R})$, i.e.,

$$\lim_{A_1, A_2, B \rightarrow \infty} \|f - C_\psi^{-1} \int_{1/A_1 \leq |a| \leq A_2, |b| \leq B} \langle f, \psi_{a,b} \rangle \psi_{a,b} \frac{dad b}{a^2}\|_{L^2} = 0. \quad (3)$$

Any function $f \in L^2(\mathbb{R})$ can then be written as a superposition of ψ_{a_k, b_ℓ} , i.e.,

$$f(x) = \sum_{k, \ell} \alpha_{k, \ell} \psi_{a_k, b_\ell}(x).$$

We refer to [13] for more details on the analysis of discrete wavelet decomposition, and, especially, for precise formulas for the coefficients $\alpha_{k, \ell}$.

Notice that from a machine learning point of view, finding the $\alpha_{k, \ell}, a_k, b_\ell$ can be thought of as a curve fitting problem, and this is how we will combine wavelet theory and machine learning techniques in our approach to modelling epidemic dynamics.

2.2 Epidemic-fitted wavelets and modelling

As we already explained in the introduction, the time development of an epidemic features local as well as global wave-type phenomena.

This leads us to the concept of epidemic-fitted wavelets. Informally speaking, such a wavelet is given by a positive real function $W : \mathbb{R} \rightarrow \mathbb{R}^{>0}$, whose value $W(t)$ at a given time t describes the number of new infected cases in a homogeneous population with respect to an epidemic that occurs in one wave only and thus will satisfy some sort of homogeneous compartmental model (without network structure).

Since we are interested in the daily infected cases, we can assume that $W(t)$ is strictly positive but tends to 0 when t tends to $\pm\infty$. Setting $w(t) = \ln W(t)$ so that $W(t) = e^{w(t)}$, the (multiplicative) growth rate of W is its log-derivative:

$$\frac{\dot{W}(t)}{W} = \dot{w}(t).$$

We wish $W(t)$ to 'start' at $t = a$, (reach its) 'peak' at $t = \chi$, and 'stop' at $t = b$ ($a < \chi < b$). This is to say that $w(a) = w(b) = 0$, $\dot{w}(\chi) = 0$, $\dot{w}(t) > 0$ for $t < \chi$ and $\dot{w}(t) < 0$ for $t > \chi$.

Definition 2 *Given an interval $(a, b) \subset \mathbb{R}$, $a \geq 0$, an epidemic-fitted wavelet is a positive real function $\psi \in L^1((a, b), \mathbb{R}^+)$ such that ψ has start-peak-stop behavior, i.e. ψ satisfies $\lim_{x \rightarrow a^+} \psi(x) = \lim_{x \rightarrow b^-} \psi(x) = 0$, and ψ admits its maximum at some point in (a, b) .*

We can interpret ψ as a wavelet $\tilde{\psi}$ in the of Definition 1 by simply setting $\tilde{\psi}(x) := \psi(x)$ for $x \in (a, b)$, $\tilde{\psi}(x) := -\psi(|x|)$ for $x < -a$, and $\tilde{\psi}(x) = 0$ otherwise. Indeed, this definition implies that $\int_{\mathbb{R}} \tilde{\psi}(x) dx = 0$ and $\int_{\mathbb{R}} |\tilde{\psi}(x)|(1 + |x|) dx < \infty$, hence $C_{\tilde{\psi}} < \infty$ by Lemma 1 and $\tilde{\psi}$ is a wavelet.

First examples of EF wavelets which come to mind are polynomial functions of degree 3 (restricted to some finite interval). Other examples of functions with start-peak-stop behavior are Gaussian functions, log-normal functions, Gompertz density functions

$$\psi_{b,c}(x) = bc \exp(c + bx - ce^{bx}), \quad (4)$$

and, in SIR models, the solution function giving the number of $I(t)$, the number of infectious individuals. (cf. [8]), etc.

In our applications to real data (see Section 4), we will employ log-normal functions as epidemic-fitted (EF) wavelets.

For treating an epidemic, we will concentrate on the curve of daily (reported) infected cases, denoted by $RC(t)$, and try to understand the epidemic growth based on this information.

Theorem 1 implies that our following ansatz is 'asymptotically' correct, as the number N grows to infinity. In particular, numerical simulations involving bigger and bigger numbers N will lead to better and better accuracy.

Proposition 1 (Ansatz) *A positive function (or curve) whose value is the number of infected cases at time t is representable as a finite linear combination of epidemic-fitted wavelets:*

$$RC(t) = \sum_{i=1}^N \alpha_i W_i(t, \theta_i), \quad (5)$$

where each such wavelet W_i can be obtained from a basic (mother) EF wavelet ψ by adding some parameters $\theta_i = (\theta_i^1, \dots, \theta_i^k)$.

Using this ansatz, we shall model epidemic dynamics by finding the wavelet series coefficients α_i and θ_i in the decomposition (5), when given the number of infected cases over a sufficient long time frame.

This amounts to solving a *curve fitting problem* in **machine learning**.

3 Epidemic-fitted (EF) wavelets

In this section, we introduce some epidemic models with different basic (mother) epidemic-fitted (EF) wavelets. In section 4 we show by fitting the Covid-19 data that log-normal EF wavelet models are highly compatible with the data and lead to very good forecast projections.

3.1 Gaussian EF wavelets

The standard Gaussian function is a fundamental example of a function which has start-peak-stop behavior and exponential growth:

$$\begin{aligned} \psi : \mathbb{R}^+ &\rightarrow (0, 1] \\ x &\mapsto \exp(-x^2/2). \end{aligned}$$

After dilating and translating, we obtain a general Gaussian function

$$\psi_{b,c}(x) = \exp\left(-\frac{(x-b)^2}{2c^2}\right).$$

We remark that in general $\lim_{x \rightarrow -\infty} \psi_{b,c}(x) = 0$, but for certain $b, c > 0$ we have $\psi_{b,c}(0) \ll 1$. In this case, we can simply set $\tilde{\psi}(x) = \max(\psi_{b,c}(x) - \psi_{b,c}(0), 0)$ as the corresponding Gaussian EF wavelet.

In [12] the authors fitted the data of daily reported cases with a two-wave model using the sum of two Gaussian functions. However, since these are symmetric with respect to the vertical line $x = b$, this model may be not compatible with the curve of daily cases. We will explain this point in further detail in the next section.

3.2 Log-normal EF wavelets

We define here the log-normal function, which is a Gaussian function in which the variable x is interchanged by $\log x$:

$$\begin{aligned} \psi_{b,c} : \mathbb{R}^+ &\rightarrow (0, 1] \\ x &\mapsto \exp\left(-\frac{(\log x - b)^2}{2c^2}\right). \end{aligned}$$

We then define the corresponding log-normal wavelet by extending

$$\psi_{b,c}(x) = -\exp\left(-\frac{(\log(-x) - b)^2}{2c^2}\right), \quad \text{for } x < 0.$$

Thus we can rewrite

$$\psi_{b,c}(x) = \text{sgn}(x) \exp\left(-\frac{\left(\frac{1}{2} \log(x^2) - b\right)^2}{2c^2}\right).$$

By dilating and translating, we obtain a general log-normal EF wavelet

$$\psi_{b,c,d}(x) = \exp\left(-\frac{\left(\frac{1}{2} \log(x - d)^2 - b\right)^2}{2c^2}\right).$$

Figure 1 depicts the graph of the log-normal function with scaling coefficient

$$\psi(x) = a \exp\left(-\frac{(\log x - b)^2}{2c^2}\right), x > 0.$$

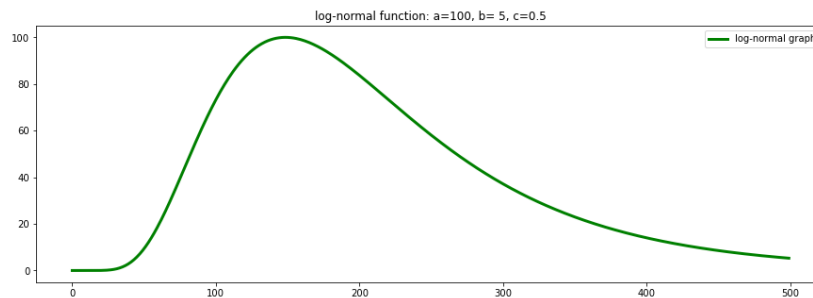


Figure 1: Log-normal graph

3.3 Further examples of EF wavelets

Based on probability distributions, we can also choose many other functions to build a basic EF wavelet.

For example, one can start here from Gompertz density functions

$$\psi_{b,c}(x) = bc \exp(c + bx - ce^{bx}), \quad (6)$$

or Beta prime density functions

$$\psi_{b,c}(x) = x^{b-1}(1+x)^{-b-c}/B(b,c), \quad (7)$$

where B is the Beta function.

For appropriately chosen parameters b, c , they all satisfy the epidemic-fitted condition in Definition 2

Another important class of EF wavelets is given by the function reporting the number of infectious individuals $I(t)$ in compartmental SIR models and their variations (such as SEIR and SIRD models, etc.)

The SIR (compartmental) model was introduced by W. O. Kermack and A. G. McKendrick [24], in which they considered a fixed population with only three compartments, and the numbers $S(t)$ (for 'susceptible'), $I(t)$ (for 'infectious'), and $R(t)$ (for 'recovered' (or 'removed')).

$$\frac{dS}{dt} = -\frac{\beta IS}{N} \quad (8)$$

$$\frac{dI}{dt} = \frac{\beta IS}{N} - \gamma I \quad (9)$$

$$\frac{dR}{dt} = \gamma I. \quad (10)$$

In Figure 2 these curves show the number of infectious individuals $I(t)$.

In general, $I(t)$ is an implicit function defined by a system of differential equations, which can lead to difficulties when trying to fit the data. However, we can here use the implicit solutions for simple SIR models which were deduced recently in [8].

3.4 Choosing suitable EF wavelets

We explain here how to choose good EF wavelets for building an epidemic model.

The first criterion to meet is the start-peak-stop behavior as discussed in Section 2.

Our second criterion is based on the following analysis of the number $I(t)$ of infectious individuals in SIR model:

$$\frac{dS}{dt} = -\frac{\beta IS}{N} \quad (11)$$

$$\frac{dI}{dt} = \frac{\beta IS}{N} - \gamma I \quad (12)$$

$$\frac{dR}{dt} = \gamma I. \quad (13)$$

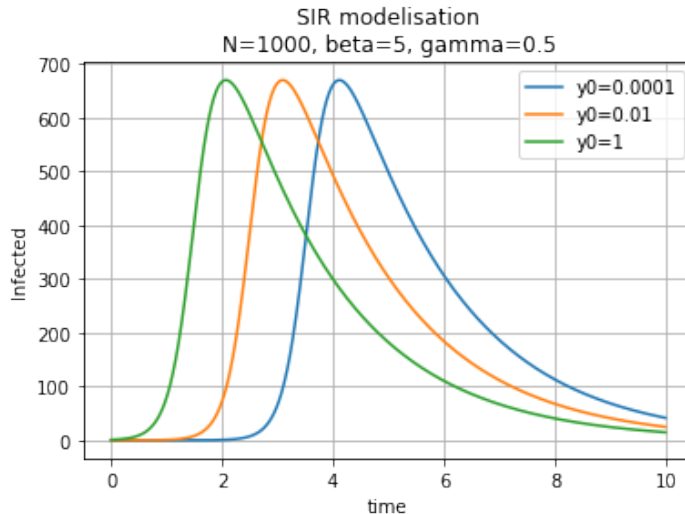


Figure 2: Infectious individuals $I(t)$ for different initial conditions

A closer look at SIR models reveals that the number $S(t)$ of susceptible individuals is decreasing in time. Therefore the number $I(t)$ of infectious also grows less and the rate of infectious, i.e., dI/dt , before the peak is always less than the one after the peak. This is an important criterion when choosing EF wavelets.

Log-normal EF wavelets actually turn out to be very good candidates in this regard:

Indeed, the first good point here is the start-peak-stop behavior, where the start for a log-normal wavelet is at $x = 0$ (or near 0), the peak is achieved at $x = e^b$ and the stop depends on the constant c . The second good one is that at the same value of ψ , the rate of the curve before the peak is less than the one after the peak.

This can be easily seen as follows. The derivative of $\psi_{b,c}$ is

$$\psi'_{b,c}(x) = \psi_{b,c}(x) \frac{-(\log x - b)}{c^2 x}. \quad (14)$$

Now suppose that $\psi(x_1) = \psi(x_2)$ with $x_1 < e^b < x_2$, then $|\log x_1 - b| = |\log x_2 - b|$. Therefore we have

$$|\psi'_{b,c}(x_1)| = \frac{x_2}{x_1} |\psi'_{b,c}(x_2)| < |\psi'_{b,c}(x_2)|$$

as required.

These are the main reasons why we first chose log normal functions as basic EF wavelets for our numerical simulations (see Section 4).

We also remark that in [34] the authors used the log-normal density function, i.e., $f_{a,b,c}(x) = \frac{a}{\sqrt{2\pi c x}} \psi_{b,c}(x)$, to fit the number of daily reported cases. However, since they used only one single function, and since there are in general many waves of the epidemic, the data may not be well-fitted enough to produce realistic projections.

4 Data-driven Numerical Forecasts

In this section, using log-normal EF wavelets we provide numerical results on the fitting and forecasting of daily new cases of Covid-19 epidemic for some European countries and US federal states.

4.1 The log-normal wavelet model

Our EF wavelet model for the curve of daily new cases is a finite representation by log-normal EF wavelet introduced in Section 4.1:

$$W(t) = \sum_{i=1}^N a_i \psi_{b_i, c_i}(t),$$

where a_i, b_i, c_i are parameters, N is the number of log-normal EF wavelets, and t is the time variable.

We intend to find the parameters a_i, b_i, c_i such that $W(t)$ is close to the daily infected number $RC(t)$ by a suitable loss function $L(\cdot, \cdot)$. In other words, we want to find parameters which minimize $L(W, RC)$.

For our numerical simulations presented in the next section of this work, we shall use the Levenberg–Marquardt algorithm (cf. [30, 37]) for the least squares loss function. The main advantage of this approach is that the loss function helps us to force the peaks of EF wavelets close to the peaks of real data.

The number of log-normal wavelets N depends on the data of each population level, since it presents the numbers sub-epidemic. In our numerical simulations, we first try with $N = 3, 5$. It would be interesting to estimate N before fitting the model. Otherwise, we will need to choose N sufficiently large, and redundant wavelets will have very small coefficients and, correspondingly, very little effect.

4.2 Data and smoothing

We will be using the data supplied by the Johns Hopkins University Center [23], noting, however, that almost all data from countries or US federal states are subject to (high) noise. One of the main reason for this is the reporting delay (cf. [7, 17]).

As explained in [17], *“there will be two main sources of delay in monitoring trends. First of all, there will be a testing delay between the actual date when an individual becomes infected and the date when that individual is ultimately tested. Second, unless test samples are very rapidly processed, there will be a further reporting delay between the date of testing and the date the test results are communicated by the reporting entity”*.

In order to reduce noise, we do smooth out the real data using a (two-sided) moving average method (cf. [36, Chapter 3], [21], [45]). A moving average is a time series constructed by taking averages of several sequential values of another time series which is a type of mathematical convolution. In statistics, two-sided moving averages are used

to *smooth* a time series in order to estimate or highlight the underlying trend. If we represent the original time series by x_1, \dots, x_n , then a (simple) two-sided moving average of the time series will be given by

$$\bar{x}_i = \frac{1}{2d+1} \sum_{k=i-d}^{i+d} x_k.$$

If the data are showing a periodic fluctuation, moving averages of equal length period will eliminate the periodic variations (cf. [36, 21]). Observing various population levels indicates that there is periodic fluctuation of 7 days on the data, and hence we will take the average of 7 days

$$\overline{RC}(i) = \frac{1}{7} \sum_{k=i-3}^{i+3} RC(k).$$

4.3 Projections and validations for the Czech Republic, France, Germany, and Italy

4.3.1 Projections from 25/10/2020

In Figures 3, 4, 5, 6, 7, 8, 9, 10, 11, the green curve shows the approximate number of daily confirmed new cases and also a possible scenario with a 60-day projection for the Czech Republic (or, in short: Czechia), France, Germany, and Italy. Other curves present log-normal EF wavelets where each one can be seen as a sub-epidemic, localised both in time and location. These EF wavelets then give us the nowcasting for the epidemic situation for each population level, i.e., forecasts present sub-epidemics, recent sub-epidemics and the combination of sub-epidemics.

For validation, we use the metric *relative percentage difference*:

$$\text{err}_i = \frac{|y_i - \hat{y}_i|}{y_i}, \quad (15)$$

where y_i is the real data at day i smoothed by 7-days moving average, \hat{y}_i is the prediction of our model.

We fit our model with the data of daily cases until 19/10 and keep last 6 days (20-25/10) for the validation set, then get the average error of 4.17% for Czechia, 7.48% for Germany and 3.25% for Italy.

Czechia				
day	real data	smoothing	prediction	error
20/10	11984	11173	10730	3.96%
21/10	14969	11710	11161	4.68%
22/10	14150	12030	11564	3.87%
23/10	15258	12689	11934	5.95%
24/10	12474	12830	12269	4.37%
25/10	7300	12295	12564	2.18%

Germany				
day	real data	smoothing	prediction	error
20/10	8523	9472	8346	11.88%
21/10	12331	10019	8763	12.53%
22/10	5952	9861	9164	7.06%
23/10	22236	10105	9545	5.54%
24/10	8688	10421	9902	4.98%
25/10	2900	9944	10231	2.88%

Italy				
day	real data	smoothing	prediction	error
20/10	10871	13322	13000	2.41%
21/10	15199	14567	14080	3.34%
22/10	16078	15934	15203	4.58%
23/10	19143	17034	16364	3.93%
24/10	19640	18266	17557	3.88%
25/10	21273	19033	18777	1.34%

However, we get an average error of 32.61% for France (see Figure 6) on the validation set from 20-25/10. We remark here that in some 3 consecutive days the total cases of France is constant in data Johns Hopkins University [23], and the total cases are updated by summing up for the day after these 3 days. For example 09-11/10 have same 732434 total cases, 16-18/10 have same 876342 total cases. This makes the daily reported cases are zero in some 2 consecutive days. Using moving average of 7 days we overcome this situation and then use the smoothing data for the projections shown in Figures 5, 6, 7.

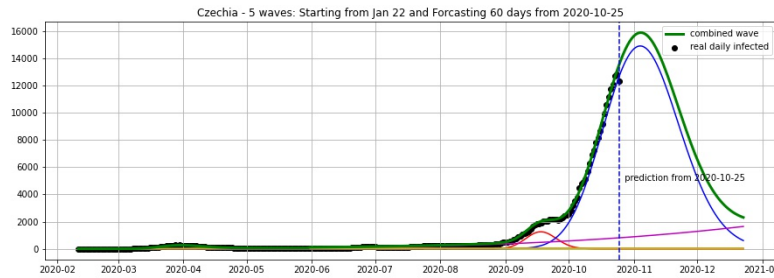


Figure 3: Czechia: fitting and forecasting from 25/10 with 5 wavelets

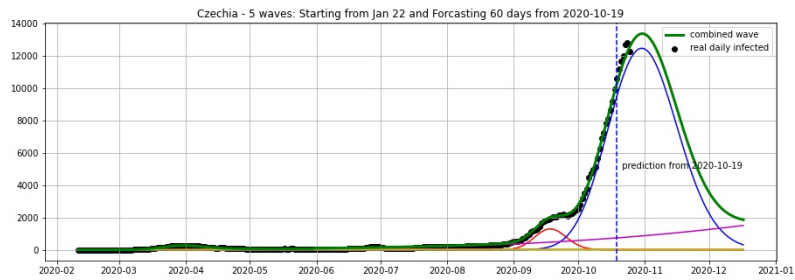


Figure 4: Czechia: fitting and forecasting from 19/10 with 5 wavelets

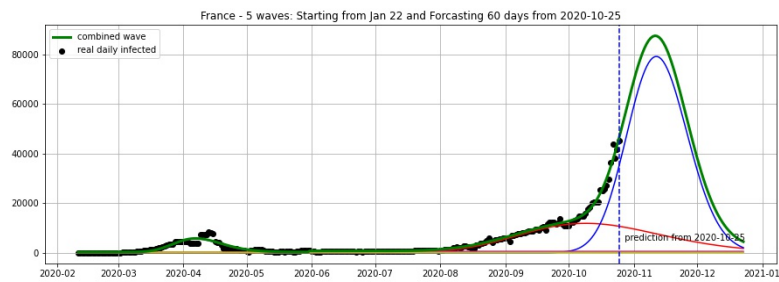


Figure 5: France: fitting and forecasting from 25/10 with 5 wavelets. Our model predicts a new wave starting from October 2020.

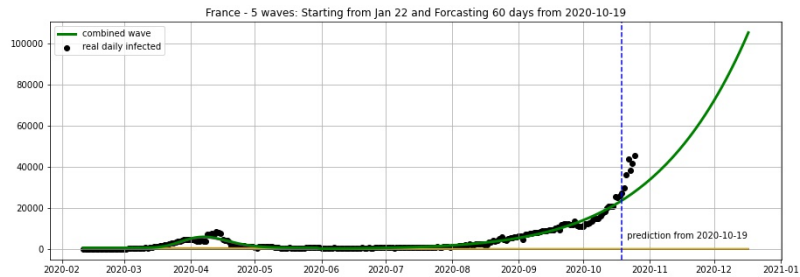


Figure 6: France: fitting and forecasting from 19/10 with 5 wavelets.

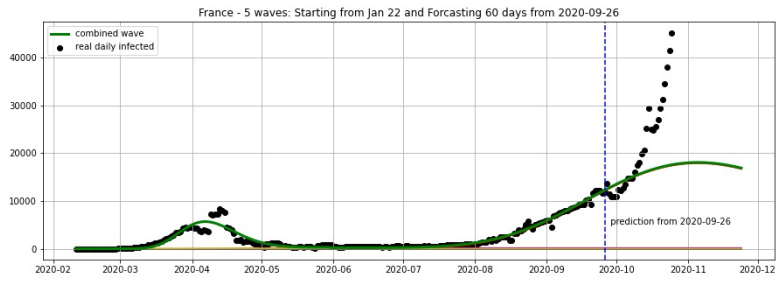


Figure 7: France: fitting and forecasting from 26/09 with 5 wavelets

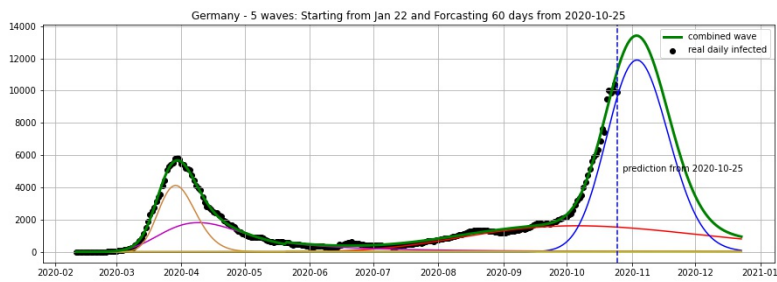


Figure 8: Germany: fitting and forecasting from 25/10 with 5 wavelets

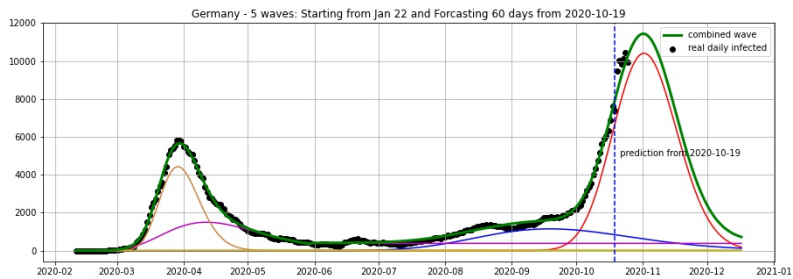


Figure 9: Germany: fitting and forecasting from 19/10 with 5 wavelets

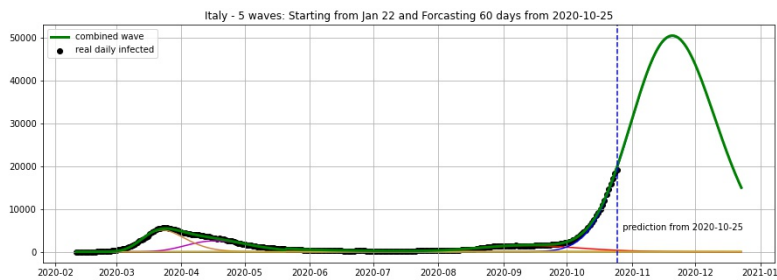


Figure 10: Italy: fitting and forecasting from 25/10 with 5 wavelets

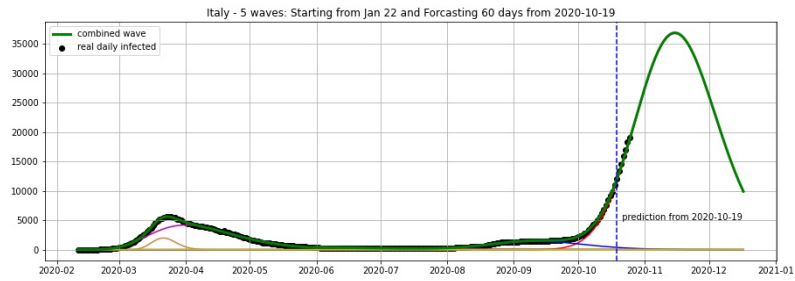


Figure 11: Italy: fitting and forecasting from 19/10 with 5 wavelets

4.3.2 Updated projections from 09/11/2020

Figures 12, 13, 14, 15 show the projection from November 09, 2020.

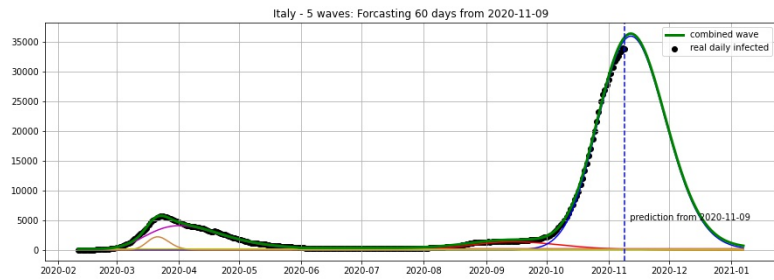


Figure 12: Italy: fitting and forecasting from 09/11 with 5 wavelets

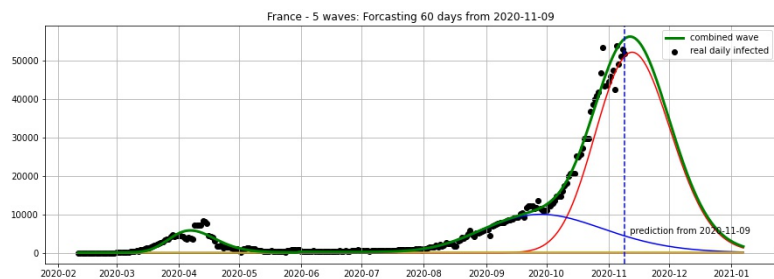


Figure 13: France: fitting and forecasting from 09/11 with 5 wavelets

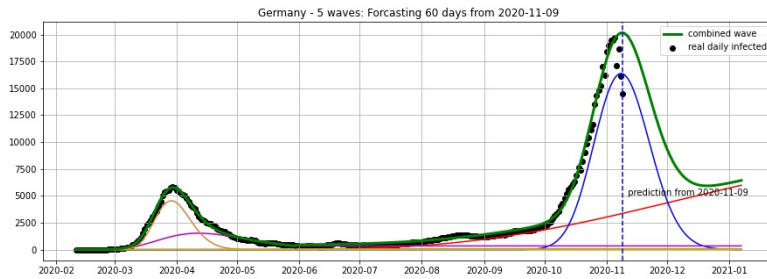


Figure 14: Germany: fitting and forecasting from 09/11 with 5 wavelets

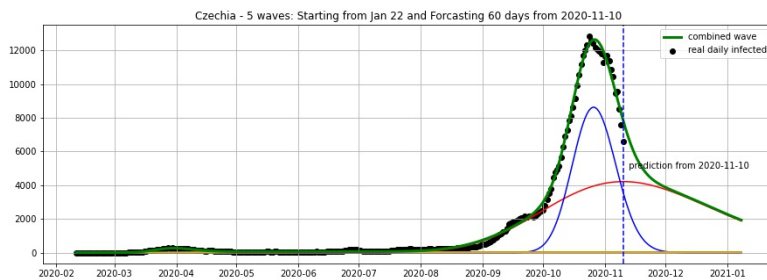


Figure 15: Czechia: fitting and forecasting from 10/11 with 5 wavelets

4.4 Projections for federal states in the United States

In Figures 16, 17, the green curve shows the projection for Florida, New York, from 25/10/2020.

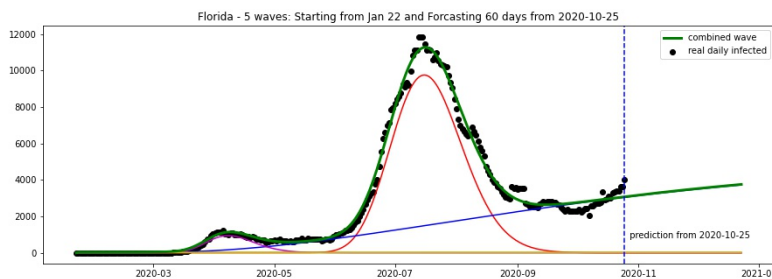


Figure 16: Florida: fitting and forecasting from 25/10

Updated projections for Florida and New York from 10/11/2020

Figures 18 and 19 show the projection for Florida, New York, from November 10, 2020.

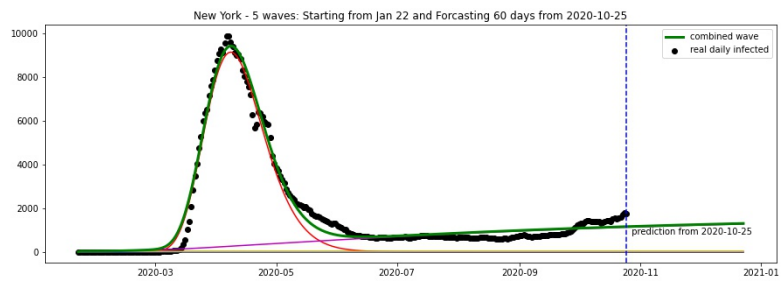


Figure 17: New York: fitting and forecasting from 25/10

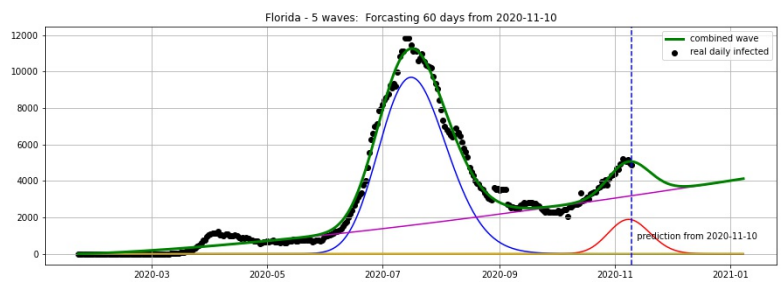


Figure 18: Florida: fitting and forecasting from 10/11/2020

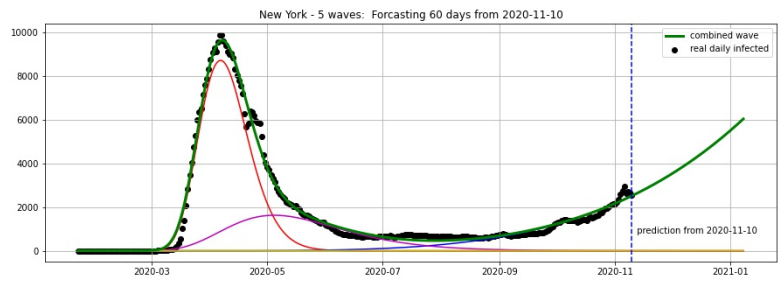


Figure 19: New York: fitting and forecasting from 10/11/2020

5 Conclusion and Outlook

(1) The numerical results in the last section of our paper suggest that our models are actually able to predict many days ahead the number of daily infected Covid-19 individuals in many different countries. In particular, our approach also gives reasonable results for the epidemic situation on population levels by precisising sub-epidemics corresponding to EF wavelets.

(2) For solving the curve-fitting problem in our model selection, we only have to use relatively few parameters. The model can be seen as a neural network containing only one hidden layer with a log-normal function activation, entailing that we do not have to deal with over-fitting problems and that the estimation error of our model is low [47, p.65].

(3) Our method of modelling of the number of daily reported cases of infectious individuals does also apply to other epidemics characteristics, e.g., to the number of active cases - and thus is also important for health care system decisions.

(4) In future work, we will present refinements of our approach as well as refinements of the curve fitting techniques employed here.

(5) In further future work, we will extend our approach based on epidemic-fitted wavelet approach to situations where EF wavelets are multivariate functions of time variables, measurement levels, or other variables such as death rate, recovery rate, etc.

References

- [1] Acuna-Zegarra M.A., Santana-Cibrian M. and Velasco-Hernandez X. J. Modeling behavioral change and COVID-19 containment in Mexico: A trade-off between lockdown and compliance, *Mathematical Biosciences*. **2020**. 325: 108370. <https://doi.org/10.1016/j.mbs.2020.108370>
- [2] Arenas A., Cota W., Gomez-Gardenes J., Gomez S., Granell C., Matamalas J., Soriano D., Steinegger B. A mathematical model for the spatiotemporal epidemic spreading of COVID19. **2020**, *MedRxiv*, doi 10.1101/2020.03.21.20040022.
- [3] Bartlett M. S. Deterministic and stochastic models for recurrent epidemics. *Berkeley Symp. on Math. Statist. and Prob.* Proc. Third Berkeley Symp. on Math. Statist. and Prob. (Univ. of Calif. Press, **1956**), 4, 81-109. <https://projecteuclid.org/euclid.bsmsp/1200502549>
- [4] Bartlett M. S. Measles periodicity and community size. *J. R. Stat. Soc. A*. **1957**, 120, 48-70.
- [5] Bertozzi A. L., et al. The challenges of modeling and forecasting the spread of COVID-19. *Proceedings of the National Academy of Sciences*. **2020**, 117 (29), 16732-16738. <https://doi.org/10.1073/pnas.2006520117>.

- [6] Brauer F., van den Driessche P., Wu J. (Eds.). *Mathematical epidemiology*. Lecture Notes in Mathematics 1945, Mathematical Biosciences Subseries. Springer-Verlag, Berlin, 2008.
- [7] Cavataio J. and Schnell S. Interpreting SARS-CoV-2 fatality rate estimates — A case for introducing standardized reporting to improve communication. *SSRN*. **2020** <https://dx.doi.org/10.2139/ssrn.3695733>
- [8] Bohner M., Streipert S., Torres D. F. M. Exact solution to a dynamic SIR model. *Nonlinear Analysis: Hybrid Systems*. **2019**, 32, 228-238.
- [9] Chowell G, Tariq A, Hyman J. A novel sub-epidemic modeling framework for short-term forecasting epidemic waves. *BMC Med*. **2019**, 17, 164. <https://doi.org/10.1186/s12916-019-1406-6>.
- [10] Chowell G., Luo R., Sun K., Roosa K., Tariq A., Viboud C. Real-time forecasting of epidemic trajectories using computational dynamic ensembles, *Epidemics*, **2020**, 30., 100379
- [11] Cotta R.M., Naveira-Cotta C.P., Magal P. Mathematical Parameters of the COVID-19 Epidemic in Brazil and Evaluation of the Impact of Different Public Health Measures. *Biology* **2020**, 9, 220.
- [12] De Noni Jr. A., et al. A two-wave epidemiological model of COVID-19 outbreaks using MS-Excel, *medRxiv*. **2020**, doi: <https://doi.org/10.1101/2020.05.08.20095133>.
- [13] Daubechies I. *Ten Lectures on Wavelets*. Society for Industrial and Applied Mathematics, 1992.
- [14] Demongeot J., Griette Q. and Magal P. SI epidemic model applied to COVID-19 data in mainland China, *medRxiv*, doi: 10.1101/2020.10.19.20214528
- [15] Guo Q., Li M., Wang C., et al. Host and infectivity prediction of Wuhan 2019 novel coronavirus using deep learning algorithm. *bioRxiv*. **2020**, doi: <https://doi.org/10.1101/2020.01.21.914044>.
- [16] Hao Y., Xu T., Hu H., Wang P., Bai Y. *Prediction and analysis of Corona Virus Disease 2019*, *PLoS ONE*. **2020**, 15(10): e0239960. <https://doi.org/10.1371/journal.pone.0239960>.
- [17] Harris J. E. *Overcoming Reporting Delays Is Critical to Timely Epidemic Monitoring: The Case of COVID-19 in New York City*, *medRxiv*. **2020**. doi: <https://doi.org/10.1101/2020.08.02.20159418>.
- [18] Hernand-Matamoros A., et al. Forecasting of COVID19 per regions using ARIMA models and polynomial functions. *Applied Soft Computing*. **2020**, 96, 106610.

- [19] Hernandez-Vargas E. A., Velasco-Hernandez, J. X. In-host Mathematical Modelling of COVID-19 in Humans. *Annual Reviews in Control* **2020**, to appear. doi: 10.1016/j.arcontrol.2020.09.006
- [20] Huang C.-Y., Chen Y.-H., Ma Y., and Kuo P.-H. Multiple-Input Deep Convolutional Neural Network 2 Model for COVID-19 Forecasting in China, *medRxiv*. **2020**. doi:<https://doi.org/10.1101/2020.03.23.20041608>.
- [21] Hyndman R.J. Moving Averages. In: Lovric M. (eds.) *International Encyclopedia of Statistical Science*. Springer, Berlin, Heidelberg, 2011.
- [22] Iboi E., Sharomi O., Ngonghala C. and Gumel A. B. Mathematical Modeling and Analysis of COVID-19 pandemic in Nigeria. **medRxiv**. **2020** . doi: 10.1101/2020.05.22.20110387
- [23] Johns Hopkins University Center, Covid-19 data: <https://github.com/CSSEGISandData/COVID-19>.
- [24] Kermack W. O., McKendrick A. G. A Contribution to the Mathematical Theory of Epidemics. *Proceedings of the Royal Society A*. **1927**,115 (772), 700-721.
- [25] Kaxiras E., Neofotistos G. Multiple Epidemic Wave Model of the COVID-19 Pandemic: Modeling Study. *J Med Internet Res*. **2020**, 22(7): e20912. doi:10.2196/20912.
- [26] Kapoor A., Ben X., Liu L., Perozzi B., Barnes M., Blais M., O'Banion S. Examining COVID-19 Forecasting using Spatio-Temporal Graph Neural Networks, *arXiv*. **2020**. <https://arxiv.org/abs/2007.03113>
- [27] Krantz P. P., Polyakov P., Rao A. S .R. S. True epidemic growth construction through harmonic analysis. *Journal of Theoretical Biology*, **2020**, 494, 110243.
- [28] Keeling M. J., Rohani P. *Modeling Infectious Diseases in Humans and Animals*. Princeton University Press, 2008.
- [29] Kucharski A. J. et al. Early dynamics of transmission and control of COVID-19: A mathematical modelling study. *Lancet Infect. Dis*. **2020** 20, 553–558 .
- [30] Levenberg K. A Method for the Solution of Certain Non-Linear Problems in Least Squares. *Quarterly of Applied Mathematics*. **1944** 2 (2): 164–168.
- [31] Liu Z., Magal P., Seydi O. and Webb G. Predicting the cumulative number of cases for the COVID-19 epidemic in China from early data. *Mathematical Biosciences and Engineering*. **2020** 17(4), 3040-3051.
- [32] Liu Z., Magal P., Seydi O. and Webb G. A COVID-19 epidemic model with latency period, *Infectious Disease Modelling* **2020** 5, Pages 323-337.

- [33] Liu Z., Magal P. and Webb G. Predicting the number of reported and unreported cases for the COVID-19 epidemics in China, South Korea, Italy, France, Germany and United Kingdom. *Journal of Theoretical Biology*, **2021** 509, 21.
- [34] Nishimoto Y., Inoue K. Curve-fitting approach for COVID-19 data and its physical background, *medRxiv*. **2020**. doi: <https://doi.org/10.1101/2020.07.02.20144899>.
- [35] Manevski D. et al. Modeling COVID-19 pandemic using Bayesian analysis with application to Slovene data. *Mathematical Biosciences*. **2020** 329. 108466
- [36] Makridakis S., Wheelwright S. C., Hyndman R. J. *Forecasting: methods and applications, 3rd edition*. Wiley, New York, 1998.
- [37] Marquardt D. An Algorithm for Least-Squares Estimation of Nonlinear Parameters. *SIAM Journal on Applied Mathematics*. **1963** 11 (2): 431–441.
- [38] Meyer Y. and Ryan D. *Wavelets: Algorithms and Applications*, Society for Industrial and Applied Mathematics, 1996.
- [39] Meyer Y. *Wavelets, Vibrations and Scalings*, (CRM Monograph Series), American Mathematical Society, 1997.
- [40] Reiner, R.C., Barber, R.M., Collins, J.K. et al. Modeling COVID-19 scenarios for the United States. **2020** *Nat Med* . doi: 10.1038/s41591-020-1132-9
- [41] Roosa K., Lee Y., Luo R., Kirpich A., Rothenberg R., Hyman J.M., Yan P., Chowell G. Real-time forecasts of the COVID-19 epidemic in China from February 5th to February 24th, 2020, *Infectious Disease Modelling*. **2020**, 5. 256-263
- [42] Saqib, M. Forecasting COVID-19 outbreak progression using hybrid polynomial-Bayesian ridge regression model. *Appl Intell* **2020**. <https://doi.org/10.1007/s10489-020-01942-7>
- [43] Soubeyrand S., Demongeot J. and Roques L. Towards unified and real-time analyses of outbreaks at country-level during pandemics. *One Health*. **2020**, 100187.
- [44] Seligmann H., Vuillerme N. and Demongeot J. Summer COVID-19 third wave: faster high altitude spread suggests high UV adaptation. *medRxiv* **2020**. DOI: 10.1101/2020.08.17.20176628
- [45] Simonoff J. S. *Smoothing Methods in Statistics, 2nd edition*. Springer-Verlag, New York, 1996.
- [46] Soper H. E. The interpretation of periodicity in disease prevalence. *J. Roy. Stat. Soc, Ser. A*. **1929**, 92, 34-61.

- [47] Shalev-Shwartz S., Ben-David S. *Understanding Machine Learning: From Theory to Algorithms*. Cambridge University Press, 2014.
- [48] Tuli S., et al. Predicting the growth and trend of COVID-19 pandemic using machine learning and cloud computing. *Internet of Things*. **2020**, 11, 100222 <https://doi.org/10.1016/j.iot.2020.100222>.
- [49] Wang J. Mathematical models for COVID-19: applications, limitations, and potentials. *Journal of Public Health and Emergency*. **2020**, 4. doi: 10.21037/jphe-2020-05.
- [50] Wang S. et al. Modeling the viral dynamics of SARS-CoV-2 infection, *Mathematical Biosciences*. **2020** 328. 108438
- [51] Wang L., Adiga A., Venkatramanan S., Chen J., Lewis B., Marathe M. Examining Deep Learning Models with Multiple Data Sources for COVID-19 Forecasting. *arXiv*. **2020**, **10**. doi: <https://arxiv.org/abs/2010.14491>
- [52] Xue L. et al. A data-driven network model for the emerging COVID-19 epidemics in Wuhan, Toronto and Italy. *Math Biosci*. **2020** 326. 108391
- [53] Yang Z., Zeng Z., Wang K., et al. Modified SEIR and AI prediction of the epidemics trend of COVID-19 in China under public health interventions. *J. of Thoracic Disease*. **2020**, 12(3):165-174. doi: 10.21037/jtd.2020.02.64.
- [54] Xiaoyong J., Yu-Xiang W. and Xifeng Y. Inter-Series Attention Model for COVID-19 Forecasting. *arXiv*. **2020**, **10**. doi: <https://arxiv.org/abs/2010.13006>

Tô Tat Dat

Centre de Mathématiques Laurent-Schwartz, École polytechnique, Cour Vaneau, 91120 Palaiseau, France and Institut de mathématiques de Jussieu – Paris Rive Gauche, Sorbonne Université, Campus Pierre et Marie Curie, 4, place Jussieu 75252 Paris, France (current adress)

email: tat-dat.to@imj-prg.fr

Protin Frédéric, Nguyen T.T. Hang, Martel Jules, Nguyen Duc Thang, Charles Piffault, Figueroa Susely

Torus Actions SAS, 3 Avenue Didier Daurat, 31400 Toulouse

email: [[@torus-actions.fr](mailto:protin;hangntt;jules;ndthang;charles.piffault;fsusely)]

Rodríguez Willy

Ecole Nationale de l'Aviation Civile, 7 Avenue Edouard Belin, 31400 Toulouse

email: willy.rodriguez@enac.fr

Hông Văn Lê

Institute of Mathematics of the Czech Academy of Sciences, Zitna 25, 11567 Praha 1, Czech Republic, email: hvle@math.cas.cz

Wilderich Tuschmann

Fakultät für Mathematik, Karlsruher Institut für Technologie (KIT), Englerstr. 2, D-76131 Karlsruhe, Germany, email: tuschmann@kit.edu

Nguyen Tien Zung
Institut de Mathematiques de Toulouse, Université Toulouse 3, email: tienzung@math.univ-toulouse.fr